Article

Residence Time Effects on Molybdenum Adsorption on Soils: Elucidation by Multi-Reaction Modeling and XANES Analysis

Wenguang Sun [1],*, Amitava Roy [2] and H. Magdi Selim [1]

[1] School of Plant, Environmental, and Soil Sciences, Louisiana State University, Baton Rouge, LA 70803, USA
[2] Center for Advanced Microstructures and Devices, Louisiana State University, Baton Rouge, LA 70803, USA
*   Correspondence: wsun3@lsu.edu

Abstract: To investigate the influence of residence time on molybdenum [Mo(VI)] adsorption behavior in soil environments, kinetic batch experiments coupled with X-ray near-edge structure (XANES) spectroscopy were performed for a neutral-pH soil (Webster loam) and two acidic soils (Mahan sand and Windsor sand) at different time scales (1 day–1 year). Batch-type experiments indicated that retention of Mo(VI) was rate limited and typical biphasic for soils. Initial rapid retention was followed by a continued slow retention with increasing aging time for Mahan and Windsor soils. In contrast, the reaction for Webster soil was nearly complete after 8 h, reflecting difference in soil properties. XANES analysis for Webster soil confirmed that most of Mo was bound to montmorillonite during long-term reaction time, whereas kaolinite constitutes a very important host phase for Mahan and Windsor soils. Sequential extraction results indicated that the percentages of Fe/Al oxide and residual fractions increased at the advanced time periods for Mahan and Windsor soils. The goodness-of-fit of numerical modeling results indicated that a simple version of multi-reaction model (MRM) with equilibrium and kinetic sorption sites was capable of describing Mo(VI) retention data for Webster loam. However, for Windsor and Mahan soils, an additional irreversible sorption site was required to simulate Mo(VI) retention over time. Although each site from MRM model cannot be unequivocally clarified from each other by either XANES analysis or sequential extraction results, their finding provided evidence of surface irreversible reactions at long residence times.

Keywords: molybdenum; adsorption; XANES; model

1. Introduction

Molybdenum (Mo) is in the second row of the transition metal elements with atomic number 42 and atomic weight of 95.94 g/mol. Mo deficiency in soils has frequently been reported as a medical trace element with essential biological functions. In addition, Mo is a potentially toxic environmental pollutant that may pose significant threat to human health, yet the current knowledge on Mo sorption in soils is limited. Mo adsorption reactions in the soil environment is a significant factor in controlling the bioavailability of this chemical element in the vadose zone [1]. The reactivity of Mo in soil environments is strongly dependent on binding affinity between Mo solution and soil reactive surfaces, such as clay minerals, soil organic matter (SOM), and metal (hydr) oxides [2–8]. Clay minerals were regarded as the most important soil components governing Mo sorption on soils. Understanding Mo sorption is important both for concerns regarding environmental contamination, and also nutrient availability in soils.

Previous studies demonstrated that retention of Mo is often kinetically controlled by residence time in soils and sediments. Kinetic studies of the batch-type [9], column [10], and stirred-flow

experiments [11] demonstrated that the adsorption of Mo by soils was rate limited and show a typical two-phase reaction process, where there is rapid adsorption in the first few minutes followed by a slow retention which may be extended for months. The kinetics of Mo are governed by the combined effects of Mo retention reactions and dynamic Mo speciation in soil. However, there is limited study of the long-term effects on Mo sorption in soils and soil components.

Several spectroscopic studies (XANES spectroscopy and Extended X-ray Absorption Fine Structure spectroscopy (EXAFS)) investigated Mo chemical speciation for reaction processes in relatively short time (up to 7 days). For example, based on XANES, Gustafsson and Tiberg [12] found that the added Mo(VI) was not reduced on sorption, although the coordination of organic-rich acid soils was altered from tetrahedral to octahedral. Arai [13] used EXAFS analysis to investigate Mo(VI) reaction mechanism at the goethite-water interface. The result further supported an inner-sphere retention mechanism which was previously demonstrated by Zhang and Sparks [8] using a pressure-jump relaxation method. However, Mo sorption mechanisms for long-term retention time (up to 1 year) has not been investigated by using XANES analysis.

Models for describing and predicting Mo retention behavior in the environment have been widely reported over the past four decades. For geochemical models, Tian et al. [14] proposed a novel unified kinetic model, which was based on the equilibrium model CD-MUSIC, to simulate cation and oxyanion adsorption and desorption processes (10 h) on ferrihydrite. A chemical equilibrium model WHAM 7 coupling with XAS analysis was successfully utilized to simulate kinetics of Zn release from soils [15]. However, such kinetic geochemical models were less successful over long-term reaction time since they failed to account for slow metal adsorption processes. The adsorption behavior of metals and metalloids need to be simulated not only on short-term (<24 h) retention studies but also on long-term (up to 1 year) sorption processes. Empirical models coupling kinetic retention and release behavior have been proven as a useful tool for describing sorption behavior of contaminants [16,17]. For example, a multi-reaction model (MRM) which considers equilibrium, kinetic reversible and irreversible retention sites has already developed to simulate heavy metals (As, Ag, Cu, Ni, and Sb) as well as nutrient (P) retention and release processes in soils [16,18–22]. However, the capability of MRM in simulating the long-term adsorption process of Mo(VI) in soils has not been investigated.

The objectives of our study were (i) to determine the time-dependent retention behavior of Mo(VI) on soils having different properties; (ii) to evaluate the capability of MRM model to simulate the long-term Mo(VI) sorption process on soils; (iii) to investigate the influence of residence time (1 day to 1 year) on Mo(VI) sorption mechanism using XANES analysis and sequential extractions.

2. Materials and Methods

2.1. Material

Three surface soils from the Ap horizon (0–10 cm) of Mahan sand, Windsor sand, and Webster loam were utilized in this study. These soil samples having different properties were collected in different locations of the USA. Specifically, Mahan sand is a fine-silty, weak acidic soil formed in iron-rich clayey, and was sampled from marine sediments. Windsor sand is a fine sandy loam formed on glacial outwash plains, and deltas of the U.S northeast region and was collected from Lebanon, New Hampshire. Webster loam formed in glacial till or local alluvium derived from the till on uplands and found in Story County, Iowa. All three soils were air-dried and passed through a 2-mm sieve before use. The soil was analyzed for pH using 1:1 soil/water paste, for total organic carbon (TOC) by wet combustion methods with gravimetric determination of CO_2 [23,24], for cation exchange capacity (CEC) by exchange with 0.1 M $BaCl_2$-0.1 M NH_4Cl, for free iron oxides by the dithionite-citrate-bicarbonate method [25], and for active iron oxides by ammonium oxalate extractions method [26,27]. Sand content was determined by wet- and dry-sieving; clay content was determined by the pipette method [28]; and silt content was determined by difference. The mineral composition of the clay-fraction particles was determined by X-ray diffraction (XRD) analysis. These soils contain very little Mo and their

physical, chemical, and mineralogical properties (e.g., pH, TOC, Fe, and Al oxides) are provided in Table 1.

Table 1. Selected physical and chemical properties of the soils studied.

Soil	Webster	Windsor	Mahan
pH	6.92	6.11	6.10
TOC [a] (%)	4.03	2.03	1.37
CEC [b] (cmol kg^{-1})	27.0	2.0	7.0
CaCO$_3$ (%)	3.7	-	-
Mo (mg kg^{-1})	0.52	0.93	0.59
Sand [c] (%)	39	77	49
Silt (%)	39	20	20
Clay (%)	22	3	31
Clay mineralogical composition [d]	Smectite (73%), Quartz (11%), Kaolinite (9%), Illite (7%)	Illite (33%), Kaolinite (29%), Chlorite (15%), Smectite (12%), Quartz (10%)	Kaolinite (75%–85%), Mica (5%–10%), Vermiculite (5%), Interlayered, Interstratified (5%–10%)
Selective extraction by Ammonium oxalate (pH 3.0)			
Fe (g kg^{-1})	0.98	0.36	0.46
Al (g kg^{-1})	0.89	0.69	0.22
Citrate-bicarbonate-dithionite (CBD)			
Fe (g kg^{-1})	4.42	3.68	6.07
Al (g kg^{-1})	0.77	3.65	3.65

[a] TOC = total organic carbon. [b] CEC = cation exchange capacity. [c] Grain size distribution: sand (2.00–0.05 mm), silt (0.05–0.002 mm), and clay (<0.002 mm). [d] percentage of mineral present.

2.2. Kinetic Batch Experiments

To investigate the rate-limited Mo(VI) sorption, kinetic batch-type experiments were carried out at constant room temperature. In these experiments, an initial 100 mg L^{-1} Mo(VI) (as Na$_2$MoO$_4$) in 0.005 M NaNO$_3$ background solutions was equilibrated in Mahan, Windsor, and Webster soils, which was higher than that used in previous sorption experiments. Such high Mo concentration was necessary to assure sufficient metal loading and an adequate XANES signal [29]. Based on the CHEAQS PRO [30], the deprotonated molybdenum oxyanion, MoO$_4$$^{2-}$ (>99%) species predominates at near-neutral pH [13,31]. For each experiment, 3-g air-dry soil in triplicates was mixed with 30-mL solution in a 40-mL high-speed centrifuge tube. The pH of the suspensions were adjusted to pH 6.9 for Webster soil and pH 6.1 for Mahan and Windsor soils. These pH values corresponded to the original pH of respective soils. These tubes were continuously shaken at 150 *g* using an orbital shaker for 8 h, 1 day, 7 days, 30 days, 45 days, 120 days, 180 days, and 1 year, respectively. The mixtures were centrifuged for 10 min at 5000× *g* before sampling and then passed through 0.45-µm membrane filter papers. Subsequently, the filtrate was analyzed using inductively coupled plasma atomic emission spectrophotometry (ICP-AES). Moreover, during the adsorption reaction period, the pH of the mixture was monitored with a standard multi-pH/millivolt meter and it was adjusted manually every 7 days by adding various amounts of acid (as 0.1 M HCl) or base (as 0.1 M NaOH) to maintain the original soil pH values. The amount of Mo(VI) sorbed were calculated from the difference between input and finial Mo concentrations in the solution phase. The residual soil samples were separated into two equal parts of 1 kg each and then stored at +5 °C for XAS (X-ray absorption spectroscopy) measurements and sequential extraction experiments.

2.3. Sequential Extractions

A four step sequential extraction method was utilized to quantify speciation of Mo in different soil aged samples from batch-type experiments. This procedure included four fractions; weakly sorbed [extraction by 0.05 M (NH$_4$)$_2$SO$_4$], strongly sorbed [0.05 M (NH$_4$)H$_2$PO$_4$], bound to Fe and Al oxides bound (0.2 M NH$_4$-oxalate buffer and 0.1 M ascorbic acid; pH 3.25), and residual (4 M HNO$_3$), respectively. Both weakly and strongly sorbed phases were measured by shaking duplicate 50-mL centrifuge tubes containing 1 g of soil in 25 mL of extractant for 24 h according to method of

Okkenhaug et al. [32]. The first two fractions were obtained by mixing 1 g soil with 25 mL of the extractant solution, shaking for 16 h, and centrifuging. The oxalate extraction step was conducted for 30 min in a water basin at 96 ± 3 °C in the light. After each extraction step, the sample was washed using deionized water and the subsequent extractions step commenced. Total Mo of the supernatant was analyzed using ICP-AES.

2.4. Mo K Edge XANES Analysis

XAS samples (1 day, 7 days, 45 days, 180 days, and 1 year for Mahan, Windsor, and Webster soils) were prepared using the methods described in the batch-type experiments. Molybdenum K-edge (20,000 eV) XANES data were collected on beam line of the J. Bennett Johnston, Sr., Center at Advanced Microstructures and Devices (CAMD), Louisiana State University campus. The beam line operated a synchrotron at 1.3 GeV and at currents between 50 and 100 mA. The continuous synchrotron X-ray was equipped with a Ge (220) double crystal monochromator. All measurements were performed in fluorescence mode using a Canberra 13-element high-purity Ge array fluorescence detector. The spectra analysis for aged soils and standard samples have been documented elsewhere [9], but here we give further details on linear combination fitting (LCF) procedure. A LCF approach was utilized to investigate the weighted combinations of aged samples spectra from the following five different standards: Mo complexed to ferrihydrite, Mo adsorbed to aluminum hydroxide [Al(OH)$_3$], Mo adsorbed to montmorillonite, Mo adsorbed to kaolinite, and Mo complexed to fulvic acid. Specifically, LCF analysis was performed over the energy range between −20 and 80 eV relative to E$_0$, and individual fractions were also constrained to the range of 0%–100%. In addition, fits were accepted only in cases when the weighting fractions summed to 100% ± 10%, and fractions were renormalized to a sum of 100% [33,34]. A standard was included in the fit only if it made an improvement of fit according to Athena, and the fit quality was judged on the basis of R-factor value [R = $\sum$(data fit)^2/$\sum$(data)^2] [35,36]. If a component was not included, it means the fits were not improved.

2.5. Multi-Reaction Model

The kinetic multi-reaction model (MRM) developed by Selim [37] was utilized to describe and predict the adsorption of Mo (VI) in the natural systems. The model assumes that a fraction of the total sorption sites is rate limited whereas the remaining fractions interact rapidly or instantaneously with Mo (VI) in solution. It also considers multiple irreversible retention reactions as concurrent and consecutive type (Figure 1). Specifically, the model can be described in the following equations:

$$\text{Reversible Kinetic} \quad \frac{\partial S_k}{\partial t} = k_1 \frac{\theta}{\rho} C^n - k_2 S_k, \tag{1}$$

$$\text{Equilibrium} \quad S_e = K_e \frac{\theta}{\rho} C^n, \tag{2}$$

$$\text{Consecutive irreversible} \quad \frac{\partial S_s}{\partial t} = k_3 S_k, \tag{3}$$

$$\text{Concurrent irreversible} \quad \frac{\partial S_i}{\partial t} = k_i \frac{\theta}{\rho} C. \tag{4}$$

In this model, C is the Mo concentration in solution (mg L^{-1}), S_e represents the amount of Mo sorbed on equilibrium phase (mg kg^{-1}), S_k represents the amount of Mo sorbed on kinetic-type phase (mg kg^{-1}), and S_s and S_i are the amount of Mo sorbed by consecutive and concurrent irreversibly phases (mg kg^{-1}), respectively. K_e is a dimensionless equilibrium constant, k_1 and k_2 (h^{-1}) are the forward and backward reaction rates linked with kinetic sites, respectively, k_3 (h^{-1}) is the irreversible rate coefficient linked with the kinetic consecutive irreversibly sites, k_i (h^{-1}) is the irreversible rate coefficient linked with Mo solution, n is the dimensionless reaction order, θ is the soil water content (cm^3 cm^{-3}), ρ is the soil bulk density (g cm^{-3}), and t is the reaction time (h). The total amount sorbed S (mg kg^{-1}) is defined as

$$S = S_e + S_k + S_s + S_i. \tag{5}$$

The model MRM was fit to the kinetic data using a nonlinear, least-squares optimization method. Numerical results were performed with the data which were best fitted, that is, those that provided the highest coefficients of determination r^2 and the lowest root-mean-square error (RMSE).

$$RMSE = \sqrt{\frac{Rss}{Nobs - Npar}}, \tag{6}$$

where R_{ss} is the residual sum of squares, N_{obs} is number of measurements, and N_{par} is number of fitted parameters.
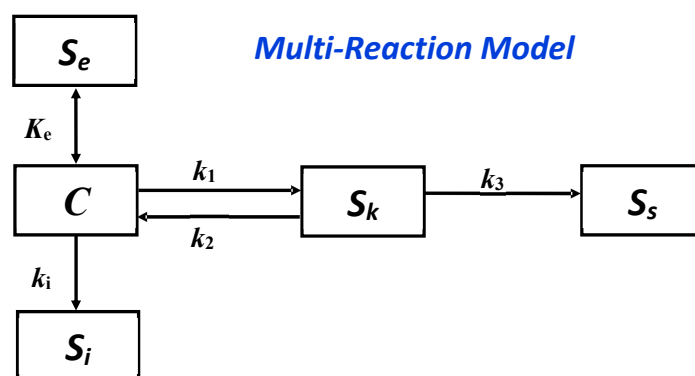

**Figure 1.** A schematic diagram of the multi-reaction model (MRM).

3. Results

3.1. Mo Sorption Kinetics

The time-dependent adsorption behaviors of Mo(VI) are shown in Figure 2 for the different soils. Batch experiments clearly indicated that retention of Mo(VI) was kinetically controlled and the initial rapid adsorption was followed by a continuous slow process lasting for months for all soils. This biphasic reaction phenomenon has been successfully reported for Mo(VI) sorption on soils and soil components at different reaction times (minutes to years) [8,9,38–40]. The adsorption of Mo(VI) at a range of concentrations (5–100 mg L^{-1}) with different soils have also been reported to show typical biphasic reaction kinetics [9,41]. Rate-limited sorption of Mo(VI) may be due to (i) different types of surface complexes (e.g., out sphere, inner sphere) can be formed on the soil matrix at high or low surface coverage. This heterogeneity of sorption sites may contribute to observed retention kinetics where retention preferentially takes place on sites with relatively high binding affinity followed subsequently by slow reaction on low retention affinity phase; (ii) diffusion of aqueous metal ion to soil reactive site is likely a kinetically controlled step of sorption reaction [16].

Adsorption for Webster soil was nearly completed (e.g., equilibrium) after 8 h, and as time increased, there was only a slight increase for the total amount of Mo(VI) sorption. However, because of low sorption capacity, there was still much Mo(VI) left in solution to sorb at the later time periods, and only 20% of the added Mo(VI) sorbed to the Webster soil after 1 year. For comparison, Mo(VI) adsorption in Mahan and Windsor soils was more kinetic than that in Webster, as indicated by the continued increase of the amounts sorbed with residence time (days to months) (Figure 2). Initial sorption was very rapid; total sorption increased over time, and after 1 year, 97% sorption occurred. The difference of sorption capacity for three soils could be explained by differences of soil properties (Table 1). Generally, high iron and aluminum oxide content, clay fraction and organic matter content, and low pH increase the sorption of Mo on soils [2,4,7,8,42,43]. Soil solution pH is a dominant factor controlling Mo

adsorption for different soil components, such as SOM, Fe/Al oxide, and clay mineral [44,45]. Brinton and O'-Connor [44] and Goldberg [45] found that the maximum of Mo adsorption on oxides capacity was observed at pH 4, and sorption decreased with increasing pH above 4. Recently, Sun and Selim [10] found that the amount of Mo sorbed and kinetic rate of an acidic soil was significantly greater than that of a neutral soil. It is believed that the maximum of anions sorbed takes place at pH value near its dissociation constant (pK). We also found that there are no significant differences of Mo adsorption rate between Windsor and Mahan soil systems. This was not surprising since Webster is a neutral soil in the presence of carbonates whereas Windsor and Mahan are acidic soils. Therefore, higher Mo sorption is expected in the two acidic soils. Moreover, Goldberg et al. [2] found that Mo adsorption on a weight basis on clay mineral was less than adsorption on Al and Fe oxides. Similar behavior was also observed by Jones [4]. This might explain the highest Mo sorption rate that was observed on both Windsor and Mahan soils.
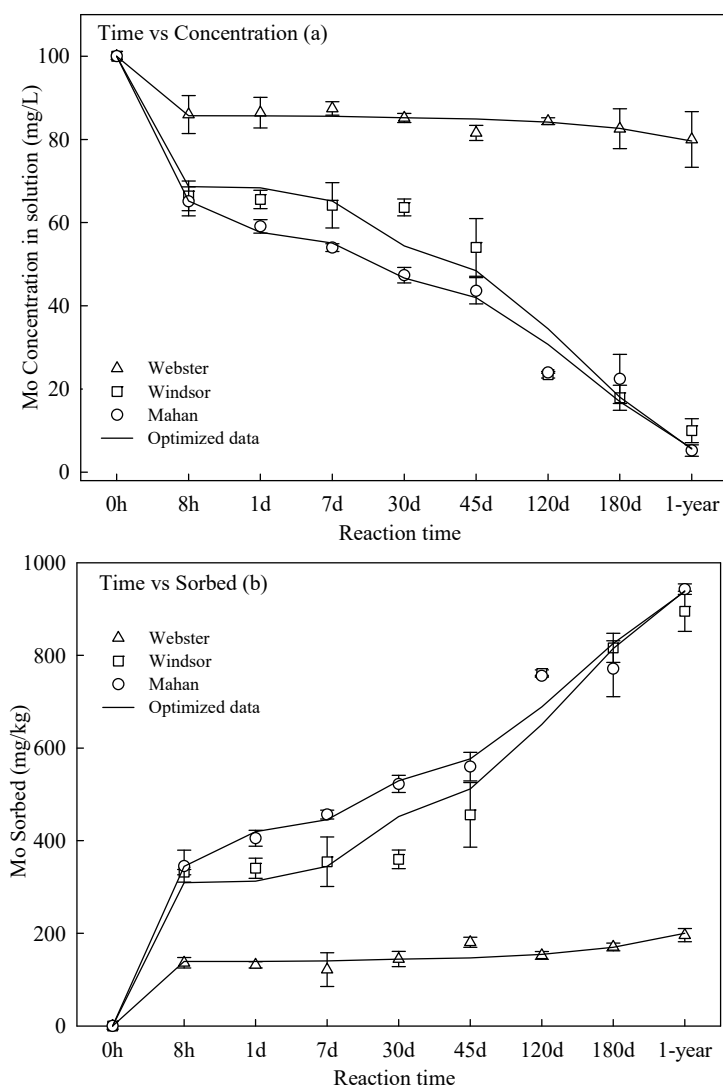
Figure 2. Adsorption kinetics of molybdenum (VI) in Mahan, Windsor, and Webster soils. (**a**) Molybdenum (VI) concentration in solution as a function of reaction time during adsorption process; (**b**) molybdenum (VI) sorbed as a function of reaction time during adsorption process.

3.2. Multi-Reaction Modeling and Reaction Mechanisms

Chemical two-phase sorption may be best predicted by two site kinetic models where a part of total sorbed is considered to occur fast and another part is kinetically controlled. Assuming a typical

biphasic Mo(VI) reaction on all soils, the two-site MRM model with three optimized parameters K_e, k_1, and k_2 was utilized to simulate the kinetic adsorption data. Numerical simulations suggest that the two-site kinetic MRM considering both equilibrium site (S_e) and kinetic site (S_k) accurately reflect the results of batch experiments for all three soils, as indicated by high correlative coefficient (R^2) values and low RMSE. The goodness-of-fit results clearly show that the adsorption kinetic rate of Mo(VI) on Mahan and Windsor soils was faster than that on Webster soil. As we demonstrated above, the difference between pH of Mahan and Windsor soil (6.1) and Webster soil (6.9) could be utilized to partially explain its higher retention rate. This is in agreement with previous findings indicating that Mo(VI) retention decreased with increasing pH.

Mobility of metals and metalloids is often kinetically controlled by residence time (i.e., reaction time) in soil environments, resulting in irreversible behaviors [29]. In order to simulate the adsorption kinetics of Mo(VI) on long-term (months–years) processes, the reactions of the consecutive and concurrent irreversible sites (S_s and S_i) was incorporated into the kinetic model. They include different types of surface precipitation that account for the formation of metal polymers, solid solution or co-precipitates, as well as homogeneous mineral precipitate. Note that in Equation (4), the concurrent irreversible sites (S_i) are a conceptual representation of direct precipitation from solution. As shown in Figure 2, Mo(VI) adsorption kinetics for Mahan and Windsor soils showed a continuous slow reaction after 1 year. We deduced that surface irreversible reactions may become a significant process influencing Mo(VI) sorption on Mahan and Windsor soils, especially at long-term residence time. Therefore, we attempted a three-site formulation of MRM where a consecutive or concurrent irreversible reaction site (S_k, S_s, and S_i) was incorporated. Modeling results showed that a three-phase mode (S_s, S_k, and S_e) caused a decrease of RMSE and improved r^2 values for both Mahan and Windsor soils (Table 2). Therefore, we concluded that the addition consecutive irreversible reaction (S_s) was required for accounting for surface complexation or precipitation reaction on soils at long-term reaction time.

Since Mo sorbed in soils is bound with the solid phase at different strengths (reversible or irreversible), a sequential extraction method was performed to evaluate residence time effect on retention affinity between Mo(VI) and the soil reactive surface on for aged samples (1 day, 7 days, 45 days, 180 days, 1 year) (Figure 3). Four fractions from weakly sorbed to residual are operationally defined. In terms of increasing Mo(VI) binding strength, adsorption of the initial fractions is readily leachable and regarded as weakly sorbed (F1), while Mo(VI) retention which was replaced by phosphate is of strong binding strength and regarded as strongly sorbed (F2). The strong linkage between Fe/Al oxide and Mo(VI) (F3) is required to be broken up by using ammonium oxalate extractant [10]. This is primarily because that this fraction was unlikely to be mobilized except under reduced conditions. In addition to Mo-Fe/Al oxide phases, other recalcitrant components of Mo sites were organic matter and residual, which were determined by digestion with strong acid (HNO_3) at high temperature. Surface irreversible reactions may occur when Mo(VI) was sorbed on the oxide-bounded and residual sites. Generally, ammonium oxalate and residual phases (F3 and F4) need a relatively long sorption time to reach equilibrium, and their retention capacities were more kinetically controlled than weakly and strongly sorbed fractions. For Mahan and Windsor soils, the longer the contact time from days to years, the higher increase in percentages of Fe/Al oxide and residual fractions, suggesting rate-limited reactions. This is agreement with the MRM simulation results that the percentage of nonlinear equilibrium retention sites (S_e) decrease while the kinetic reversible reaction (S_k) and irreversible sites (S_s) increase with reaction time (Figure 4). By contrast, Mo(VI) distribution on Webster soil did not change over time. Detailed model results show that the kinetic site (S_k), which clearly indicates that residence time, did not apparently affect the sorption process (Figure 4).

3.3. Mo K Edge XANES Analysis

Figure 5 shows XANES spectra of Mo(VI) aged Mahan, Windsor, and Webster samples, a 20 mM Na_2MoO_4 solution, and the standards of ferrihydrite, $Al(OH)_3$, montmorillonite, kaolinite, and fulvic acid. We investigated the long-term effects of Mo(VI) reactions by comparing XANES spectra of aged

soil samples. The intensity of pre-edge features changed with increasing aging time, indicating that Mo(VI) coordination environment could be altered with time reaction. For Windsor soil, at initial time sorption (1 day), the sample had least intense pre-edge features. However, the feature becomes more pronounced at 45-day samples. This may due to Mo being a distorted tetrahedral configuration with time reaction. It is noteworthy to mention that the less intense feature was also observed at 180 days and 1 year. Moreover, with increasing the aging time from 1 day to 1 year, there is a large change in the Mo(VI) sorbed fraction for Windsor and Mahan soil. Linear combination fitting (LCF) results indicated that, throughout the aging time from 1 day–1 year, kaolinite is the dominant species for Windsor soil (~64%–94%), followed by montmorillonite (~17%–45%) and $Al(OH)_3$ (~1%–21%) (Figure 6). It is interesting to see that the $Al(OH)_3$ and fulvic acid fraction is pronounced (~48%) at the 1 year Windsor sample, suggesting the presence of an irreversible reaction. Similar to Windsor soil, Mo sorbed onto kaolinite represented a large fraction of total soil Mo for Mahan (~47%–84%). At the later reaction time, the $Al(OH)_3$ fractions contributed only to a very small degree to the total soil Mo (~3%–7%). These results suggest that kaolinite is likely to be a very important host phase for Mo(VI) in Windsor and Mahan soils. This is agreement with the clay mineralogy analysis which both soils are highly dominated by kaolinite. For comparison, there was 97% sorbed Mo(VI) retained as montmorillonite at the 1-day Webster sample. After 1 day, the fraction of montmorillonite decreased and ranges from ~97% to ~64%. A minor part of the Mo for Webster soil was found to be bound with $Al(OH)_3$ (~2%–20%).

Table 2. Comparison of parameters and goodness-of-fit determined from fitting different MRM model formulations (M1–M9) to kinetic batch data for Webster, Windsor, and Mahan soil.

	r^2	RMSE [a]	K_e [b]	k_1	k_2	k_3	k_i
					h^{-1}		
				Mahan soil			
M1	0.375	18.10	-	4.001 ± 2.271	0.677 ± 0.445	-	-
M2	0.966	4.604	-	8.275 ± 2.073	3.087 ± 0.922	0.012 ± 0.0025	-
M3	0.973	4.040	-	8.513 ± 2.016	3.368 ± 0.949	-	0.011 ± 0.0014
M4	0.973	5.185	-	8.936 ± 2.822	3.776 ± 1.393	0.000 ± 0.0009	0.013 ± 0.0024
M5	0.962	4.430	23.267 ± 2.14	-	-	-	0.011 ± 0.0015
M6	0.961	4.843	22.91 ± 2.427	0.043 ± 0.009	0.0019 ± 0.002	-	-
M7	0.969	3.825	21.100 ± 2.67	1.056 ± 0.030	0.309 ± 0.0201	0.048 ± 0.004	-
M8	0.974	4.417	15.202 ± 10.4	1.697 ± 3.747	1.534 ± 2.309	-	0.011 ± 0.0016
M9	0.974	5.108	15.469 ± 10.3	1.583 ± 3.400	1.438 ± 2.150	0.000 ± 0.002	0.011 ± 0.0021
				Windsor soil			
M1	0.848	21.71	-	0.107 ± 0.049	0.006 ± 0.0067	-	-
M2	0.938	7.513	-	23.44 ± 2.074	9.448 ± 0.7622	0.019 ± 0.0057	-
M3	0.935	7.407	-	17.22 ± 14.07	7.383 ± 6.643	-	0.010 ± 0.0020
M4	0.234	57.16	-	1.35 ± 1470	9.835 ± 15487	0.007 ± 833.22	1.181 ± 23.51
M5	0.934	6.719	24.321 ± 3.77	-	-	-	0.010 ± 0.0019
M6	0.940	6.989	23.95 ± 4.069	0.055 ± 0.014	0.002 ± 0.0020	-	-
M7	0.937	5.469	24.39 ± 5.148	0.750 ± 0.022	0.601 ± 0.0048	0.015 ± 0.0276	-
M8	0.942	8.462	23.50 ± 4.986	0.057 ± 0.015	0.001 ± 0.0042	-	0.000 ± 0.0065
M9	0.876	26.494	4.113 ± 6912	1.828 ± 6998	15.86 ± 4381	0.00003 ± 0.27	0.019 ± 0.029
				Webster soil			
M1	0.074	2.692	-	6.994 ± 3.112	4.862 ± 2.273	-	-
M2	0.665	1.722	-	8.925 ± 6.213	7.036 ± 5.135	0.001 ± 0.0005	-
M3	0.534	105.51	-	2.539 ± 41.73	19.830 ± 0.000	-	0.000 ± 0.0115
M4	0.564	66.158	-	0.412 ± 1.779	0.029 ± 0.392	0.000 ± 0.0554	0.000 ± 0.421
M5	0.666	1.617	12.587 ± 0.71	-	-	-	0.0002 ± 0.000
M6	0.716	1.602	11.983 ± 0.93	0.065 ± 0.004	0.008 ± 0.0075	-	-
M7	0.772	1.969	11.482 ± 1.33	0.016 ± 0.022	0.043 ± 0.0835	0.005 ± 0.006	-
M8	0.770	1.663	11.45 ± 1.112	0.012 ± 0.017	0.051 ± 0.082	-	0.0002 ± 0.000
M9	0.760	2.153	11.459 ± 1.40	0.006 ± 0.012	0.026 ± 0.228	0.00003 ± 0.08	0.0001 ± 0.002

[a] RMSE = root mean square error; [b] optimized parameters with calculated standard error.
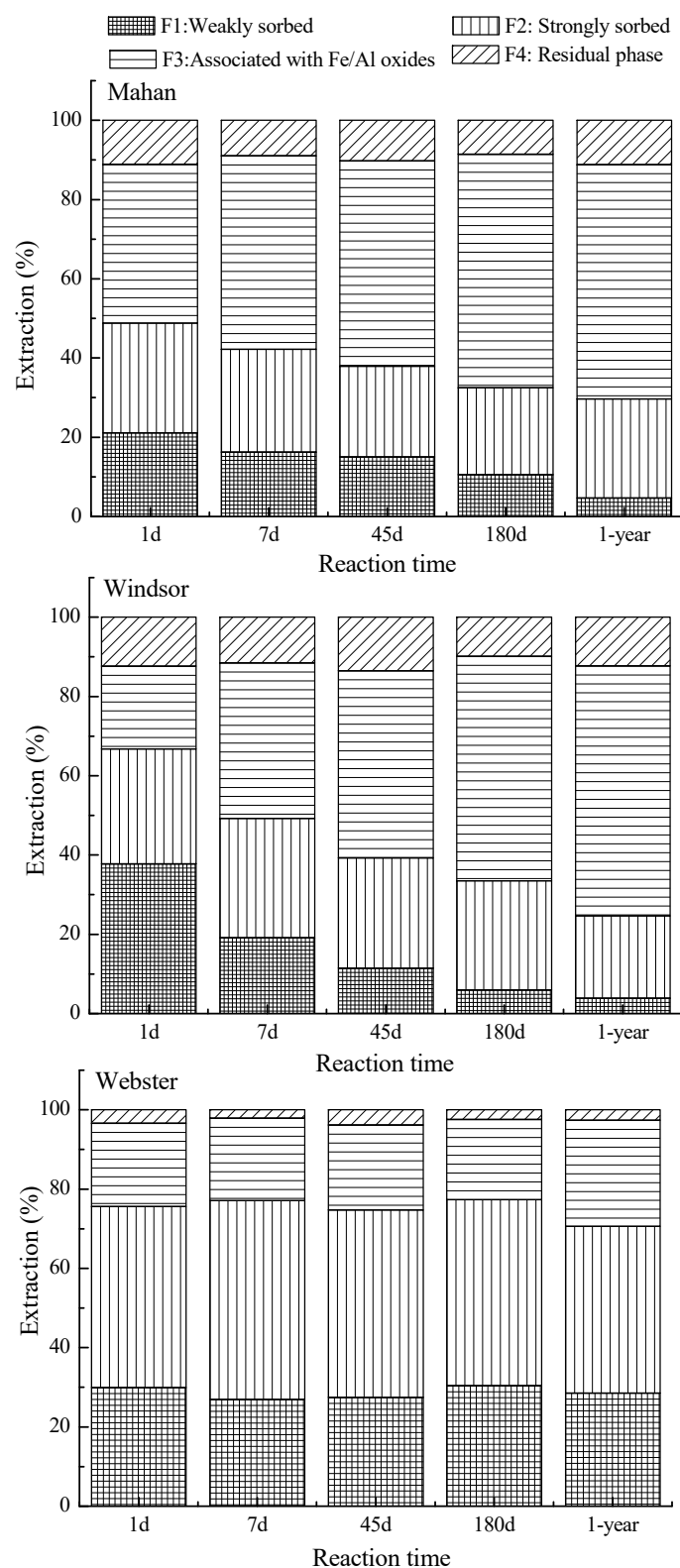
Figure 3. Distribution of molybdenum among retention phases Mahan, Windsor, and Webster soils as determined from sequential extraction. Different groups indicate different reaction time of 1 day, 7 days, 45 days, 180 days, and 1 year.
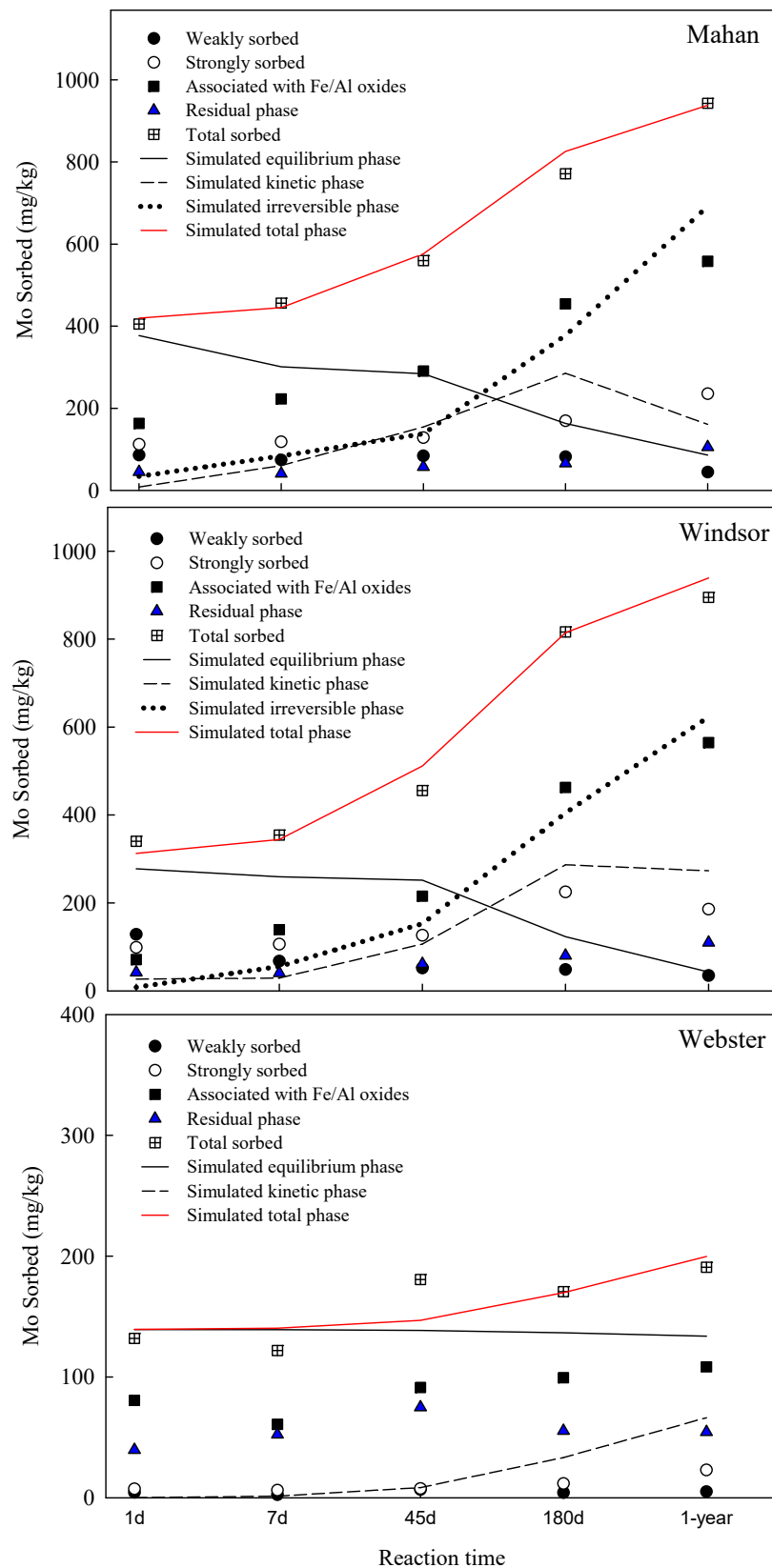
Figure 4. Total Molybdenum (Mo) sorbed by the different soils at the termination of adsorption. Data of different circles were from sequential extraction results. Dotted, solid, and dashed curves represent MRM simulation of total amount, equilibrium, and irreversible phase sorbed, respectively.
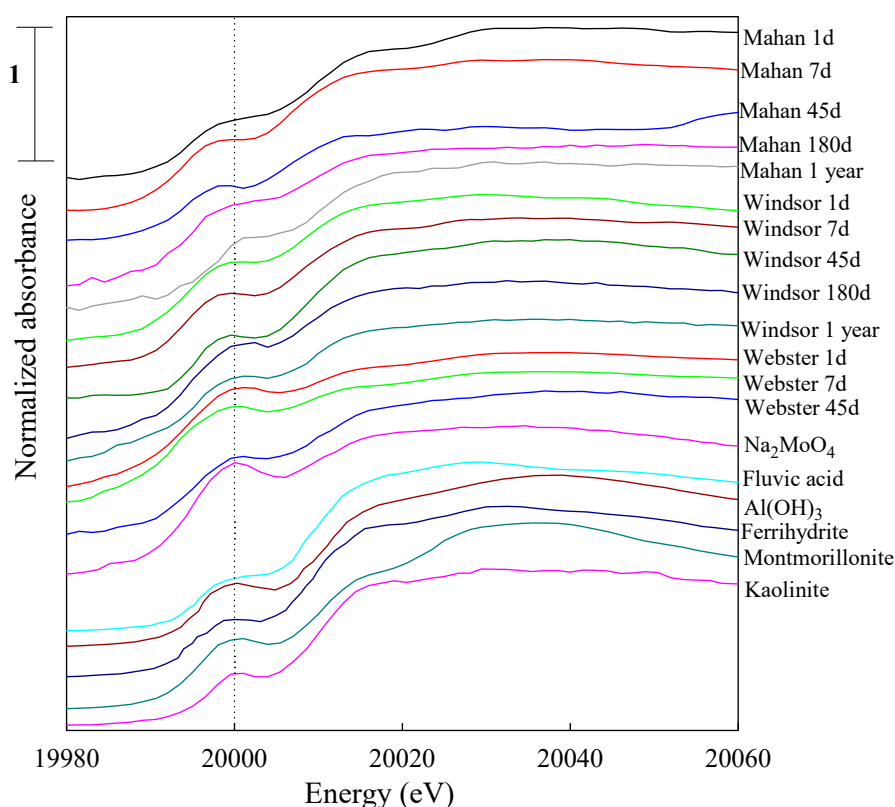
Figure 5. Mo K-edge XANES spectra of selected Mo reference compounds, Mo sorbed kaolinite, Mo sorbed to montmorillonite, Mo sorbed to Al(OH)3, Mo sorbed to ferrihydrite, Mo complexed to fulvic acid, and aged Mo reacted soils.
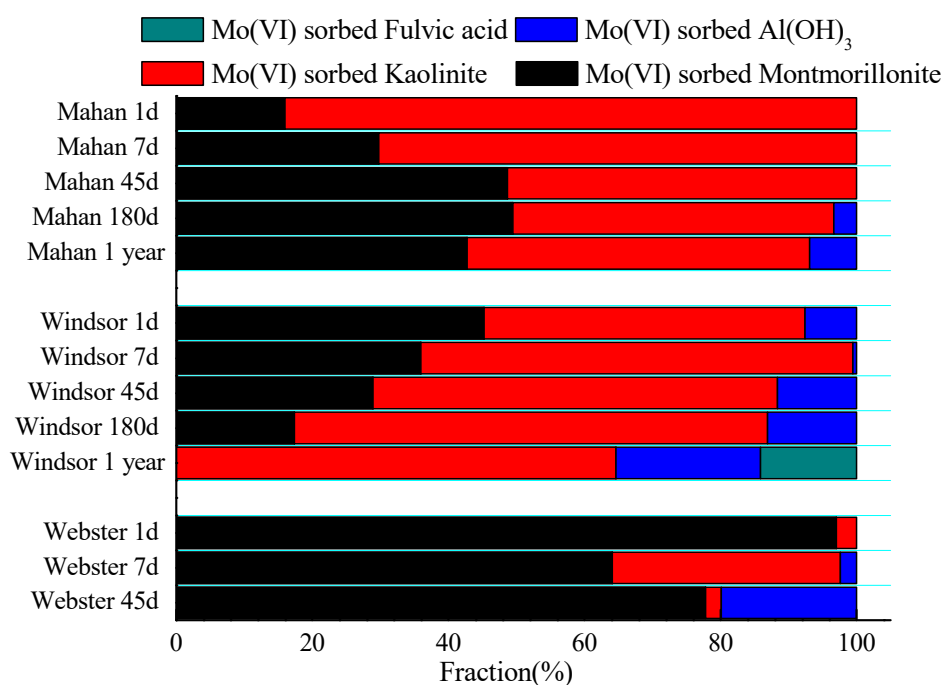
Figure 6. Mo(VI) speciation based on XANES linear combination fitting (LCF) of different reacted soils at specific times.

As stated above, the sequential extractions results indicated that the ammonium oxalate (F3, associated with Fe/Al oxides) and residual fractions (F4) comprised ~50% of the total soil

Mo(VI). XANES analysis for Windsor and Mahan soils confirmed that most of Mo was bound to kaolinite during long-term reaction time. Therefore, we deduce that these two fractions (F3/F4) are associated with phyllosilicates (e.g., kaolinite) and other recalcitrant minerals, because strong acids cannot totally dissolve phyllosilicates and silicates [36]. This indicated the surface irreversible reaction may be an important process at long residence times. This was also postulated by modeling results that an additional irreversible reaction phase was required to describe Mo(VI) retention with time. Although there are differences in Mo(VI) speciation between the sequential extractions and LCF procedures because of differences in mineralogical properties which greatly affect mineral solubility in the soil, the analysis of sequential extractions of soil samples could provide complementary information on Mo(VI) speciation for XANES analysis.

4. Conclusions

Understanding of the mechanisms of Mo(VI) retention over extended periods of months is a prerequisite to investigate the environmental risk of Mo(VI) contamination in soil and water environments. In this study, biphasic Mo(VI) adsorption was observed for three different soils. The kinetics of Mo(VI) adsorption for Webster loam was nearly complete in first 8 h; however, the reaction for Mahan and Windsor soils continued over 1 year. Linear combination fitting (LCF) of the soil XANES spectra indicated that Mo(VI)-sorbed kaolinite was an important component contributing 47%–84% and 64%–94% for Mahan and Windsor soils on long-term reaction time, respectively. This is agreement with the clay mineralogy analysis that both soils are strongly dominated by kaolinite. We deduced that Fe/Al oxide sorption and residual phases from sequential extraction experiments are associated with phyllosilicates (e.g., kaolinite) and other recalcitrant minerals, because strong acids cannot totally dissolve phyllosilicates and silicates. Both XANES analysis and sequential extraction results could be used to explain the increased irreversibility of adsorbed Mo(VI) with increasing time. Our numerical modeling results can be used to understand actual irreversible reaction process, where the percentages of equilibrium retention site decrease while the kinetic retention reaction and irreversible site increase with increasing aging time. Furthermore, sequential exaction results demonstrated a correlation between the percentage of Fe/Al oxide sorption fraction and the corresponding significance of kinetically controlled retention processes.

Author Contributions: Conceptualization, W.S. and H.M.S.; Methodology, W.S. and A.R.; Software, W.S.; Validation, W.S., A.R. and H.M.S.; Formal Analysis, W.S.; Investigation, W.S.; Resources, A.R. and H.M.S.; Data Curation, H.M.S.; Writing-Original Draft Preparation, W.S.; Writing-Review & Editing, W.S. and H.M.S.; Visualization, H.M.S.; Supervision, H.M.S.; Project Administration, H.M.S.; Funding Acquisition, H.M.S.

References

1. Gupta, U.C. *Molybdenum in Agriculture*; Cambridge University Press: Cambridge, UK, 1997.
2. Goldberg, S.; Forster, H.S.; Godfrey, C.L. Molybdenum adsorption on oxides, clay minerals and soils. *Soil Sci. Soc. Am. J.* **1996**, *60*, 425–432. [CrossRef]
3. Helz, G.R.; Bura-Nakić, E.; Mikac, N.; Ciglenečki, I. New model for molybdenum behavior in euxinic waters. *Chem. Geol.* **2011**, *284*, 323–332. [CrossRef]
4. Jones, L.H.P. The solubility of molybdenum in simplified systems and aqueous soil suspensions. *J. Soil Sci.* **1957**, *8*, 313–327. [CrossRef]
5. Pendias, K.A.; Pendias, H. *Trace Elements in Soils and Plants*, 3rd ed.; CRC Press: New York, NY, USA, 2001; pp. 260–267.
6. Sun, W.; Selim, H.M. Kinetic Modeling of pH-Dependent Molybdenum(VI) Adsorption and Desorption on Iron Oxide-Coated Sand. *Soil Sci. Soc. Am. J.* **2019**, *83*, 357–365. [CrossRef]
7. Xu, N.; Christodoulatos, C.; Koutsospyros, A.; Braida, W. Competitive sorption of tungstate, molybdate and phosphate mixtures onto goethite. *Land Contam. Reclam.* **2009**, *17*, 45–57. [CrossRef]

8. Zhang, P.C.; Sparks, D.L. Kinetics and mechanisms of molybdate adsorption/desorption at the goethite/water interface using pressure jump relaxation. *Soil Sci. Soc. Am. J.* **1989**, *53*, 1028–1039. [CrossRef]

9. Sun, W.; Selim, H.M. Kinetics of Molybdenum Adsorption-Desorption in Soils. *J. Environ. Qual.* **2018**, *47*, 504–512. [CrossRef]

10. Sun, W.; Selim, H.M. Transport and Retention of Molybdenum(VI) in Soils: Kinetic Modeling. *Soil Sci. Soc. Am. J.* **2018**, *83*, 86–96. [CrossRef]

11. Sun, W.; Selim, H.M. A General Stirred-Flow Model for Time-dependent Adsorption and Desorption of Heavy Metal in Soils. *Geoderma* **2019**, *347*, 25–31. [CrossRef]

12. Gustafsson, J.P.; Tiberg, C. Molybdenum binding to soil constituents in acid soils: An XAS and modelling study. *Chem. Geol.* **2015**, *417*, 279–288. [CrossRef]

13. Arai, Y. X-ray absorption spectroscopic investigation of molybdenum multinuclear sorption mechanism at the goethite-water interface. *Environ. Sci. Technol.* **2010**, *44*, 8491–8496. [CrossRef] [PubMed]

14. Tian, L.; Shi, Z.; Lu, Y.; Dohnalkova, A.; Lin, Z.; Dang, Z. Kinetics of cation and oxyanion adsorption and desorption on ferrihydrite: Roles of ferrihydrite binding sites and a unified model. *Environ. Sci. Technol.* **2017**, *51*, 10605–10614. [CrossRef] [PubMed]

15. Peng, L.F.; Shi, Z.; Wang, P.; Li, W.; Lin, Z.; Dang, Z.; Sparks, D.L. kinetics of Zn release from soils: Roles of soil binding sites. *J. Colloid Interface Sci.* **2018**, *514*, 146–155. [CrossRef] [PubMed]

16. Zhang, H.; Selim, H.M. Kinetics of arsenate adsorption- desorption in soils. *Environ. Sci. Technol.* **2005**, *39*, 6101–6108. [CrossRef] [PubMed]

17. Zhang, H.; Selim, H.M. Modeling the transport and retention of arsenic(V) in soils. *Soil Sci. Soc. Am. J.* **2006**, *70*, 1677–1687. [CrossRef]

18. Elbana, T.A.; Selim, H.M. Copper Mobility in Acidic and Alkaline Soils: Miscible Displacement Experiments. *Soil Sci. Soc. Am. J.* **2011**, *75*, 2101–2110. [CrossRef]

19. Elbana, T.; Selim, H. Lead mobility in calcareous soils: Influence of cadmium and copper. *Soil Sci.* **2013**, *178*, 417–424. [CrossRef]

20. Liao, L.X.; Selim, H.M. Reactivity of nickel in soils: Evidence of retention kinetics. *J. Environ. Qual.* **2010**, *39*, 1290–1297. [CrossRef]

21. Liao, L.; Selim, H.M.; DeLaune, R.D. Mercury adsorption-desorption and transport in soils. *J. Environ. Qual.* **2009**, *38*, 1608–1616. [CrossRef]

22. Zhang, H.; Li, L.; Zhou, S. Kinetic modeling of antimony(V) adsorption-desorption and transport in soils. *Chemosphere* **2014**, *111*, 434–440. [CrossRef]

23. Nelson, D.W. Carbonate and gypsum. In *Methods of Soil Analysis. Part 2. Chemical and Microbiological Properties*; American Society of Agronomy, Soil Science Society of America: Madison, WI, USA, 1982; Volume 9, pp. 181–197.

24. Nelson, D.W.; Sommers, L.E. Total carbon, organic carbon and organic matter. In *Methods of Soil Analysis. Part 2 Chemical and Microbiological Properties*; Page, A.L., Miller, R.H., Keeney, D.R., Eds.; American Society of Agronomy, Soil Science Society of America: Madison, WI, USA, 1982; pp. 539–579.

25. Chao, T.T.; Zhou, L. Extraction technique for selective dissolution of amorphous iron oxides from soils and sediments. *Soil Sci. Soc. Am. J.* **1983**, *47*, 225–232. [CrossRef]

26. Mehra, Q.P.; Jackson, M.L. Iran oxide removal from soils and days by a dithionite-citrate system with sodium bicarbonate buffer. *Clays Clay Miner.* **1960**, *7*, 317–332. [CrossRef]

27. Buchter, B.; Davidoff, B.; Amacher, C.; Hinz, C.; Iskandar, I.K.; Selim, H.M. Correlation of Freundlich Kd and n retention parameters with soils and elements. *Soil Sci.* **1989**, *148*, 370–379. [CrossRef]

28. Gee, G.W.; Bauder, J.W. Particle-size analysis. In *Methods of Soil Analysis. Part 1*, 2nd ed.; Klute, A., Ed.; Agron. Monogr. 9; ASA and SSSA: Madison, WI, USA, 1986; pp. 383–411.

29. Arai, Y.; Sparks, D.L. Residence time effects on arsenate surface speciation at the aluminum oxide-water interface. *Soil Sci.* **2002**, *167*, 303–314. [CrossRef]

30. Verweij, W. Chemical Equilibria in Aquatic Systems: CHEAQS NEXT. CHEAQS. 2010. Available online: http://home.tiscali.nl/cheaqs/index.html (accessed on 7 July 2017).

31. Sun, W.G.; Selim, H.M. Molybdenum-phosphate retention and transport in soils. *Geoderma* **2017**, *308*, 60–68. [CrossRef]

32. Okkenhaug, G.; Zhu, Y.-G.; Luo, L.; Lei, M.; Li, X.; Mulder, J. Distribution, speciation and availability of antimony (Sb) in soils and terrestrial plants from an active Sb mining area. *Environ. Pollut.* **2011**, *159*, 2427–2434. [CrossRef] [PubMed]

33. Thompson, A.; Attwood, D.; Gullikson, E.; Howells, M.; Kim, K.-J.; Kirz, J.; Kortright, J.; Lindau, I.; Pianetta, P.; Robinson, A.; et al. *X-ray Data Booklet*; Lawrence Berkeley National Laboratory, University of California: Berkeley, CA, USA, 2009.

34. Larsson, M.A.; Hadialhejazi, G.; Gustafsson, J.P. Vanadium sorption by mineral soils: Development of a predictive model. *Chemosphere* **2017**, *168*, 925–932. [CrossRef]

35. Calvin, S. *XAFS for Everyone*; CRC Press: Boca Raton, FL, USA, 2013.

36. Wisawapipat, W.; Kretzschmar, R. Solid phase speciation and solubility of vanadium in highly weathered soils. *Environ. Sci. Technol.* **2017**, *51*, 8254–8262. [CrossRef]

37. Selim, H.M. *Transport & Fate of Chemicals in Soils: Principles & Applications*; CRC Press: Boca Raton, FL, USA, 2014.

38. Kim, M.J.; Jang, M. Adsorption of molybdate onto hematite: Kinetics and equilibrium. *Water Geosci.* **2010**, *30*, 170–173.

39. Lang, F.; Pohlmeier, A.; Kaupenjohann, M. Mechanism of molybdenum sorption to iron oxides using pressure-jump relaxation. *J. Soil Sci. Plant Nutr.* **2000**, *163*, 571–575. [CrossRef]

40. Vistoso, G.E.M.V.; Bolan, N.S.; Theng, B.K.; Mora, M. Kinetics of molybdate and phosphate sorption by some Chilean Andisols. *J. Soil Sci. Plant Nutr.* **2009**, *9*, 55–68. [CrossRef]

41. Matern, K.; Rennert, T.; Mansfeldt, T. Molybdate adsorption from steel slag eluates by subsoils. *Chemosphere* **2003**, *93*, 2108–2115. [CrossRef] [PubMed]

42. Lang, F.; Kaupenjohann, M. Immobilisation of molybdate by iron oxides: Effects of organic coatings. *Geoderma* **2003**, *113*, 31–46. [CrossRef]

43. Vistoso, E.; Theng, B.K.G.; Bolan, N.S.; Parfitt, R.L.; Mora, M.L. Competitive sorption of molybdate and phosphate in Andisols. *J. Soil Sci. Plant Nutr.* **2012**, *12*, 59–72. [CrossRef]

44. Brinton, S.R.; O'-Connor, G.A. Sorption of molybdenum in soils field-equilibrated with biosolids. *Commun. Soil Sci. Plant Anal.* **2003**, *34*, 1331–1346. [CrossRef]

45. Goldberg, S. Influence of soil solution salinity on molybdenum adsorption by soils. *Soil Sci.* **2009**, *174*, 9–13. [CrossRef]